Tidal Disruption of Elliptical Galaxies in Rich, High-Redshift HST Clusters

by

WILLIAM LEO KISSINGER

A THESIS

Presented to the Department of Physics
and the Robert D. Clark Honors College
In partial fulfillment of the requirements for the degree of
Bachelor of Science

Spring 2023

Abstract

William Leo Kissinger for the degree of Bachelor of Science
in the Department of Physics to be taken June 2023

Title: Tidal Disruption of Elliptical Galaxies
in Rich, High-Redshift HST Clusters

Approved: James M. Schombert, Ph.D.
Primary Thesis Advisor

Elliptical galaxy structure is widely considered to be homogenous. While they do vary in ellipticity and shape, their structure is not so varied. Or so was believed until 2015 when Schombert noticed in a study of field ellipticals that a significant percentage deviated from typical structure. These D ellipticals, as he called them, are more diffuse than traditional ellipticals. This is shown by having shallower surface luminosity profiles than the template of the same magnitude that fits normal ellipticals. In this project I have used a similar process of template fitting on galaxies within CLASH cluster environments to determine if this phenomenon exists there as well. I found that there are indeed galaxies with shallow profiles, but there is also a selection with steeper profiles. I hypothesize that the steep profiles are the result of galaxy mergers, explaining why they did not appear in the field, and that shallow profiles come from ellipticals gaining kinetic energy from interactions with the cluster's potential well caused by elongated orbits. I also found that the templates are not a perfect match for the cluster environment but are useful for identifying tidally truncated galaxies.

Acknowledgements

I would like to thank Dr. James Schombert for helping me come up with this thesis project and for remaining such an integral part of the process throughout.

I would also like to thank Dr. Lisa Munger for serving on my committee.

Finally, I thank all of my friends who put up with my ramblings about this project. I would not have been able to complete this work without each of them providing their own type of support.

Thank you all.

Table of Contents

1 Introduction **1**

1.1 Elliptical Structure 1

1.2 Templates and Color Filters 2

1.3 Anomalous Ellipticals 4

1.4 Cluster Ellipticals 6

1.5 Mergers 7

2 Methods **8**

2.1 Data Set and Acquisition 8

2.2 Individual Galaxies 10

2.3 Plotting and Fitting 12

2.4 Templates and Categorization 13

3 Discussion **21**

3.1 Results 21

3.2 Merger Formation and Steep Profiles 23

3.3 Shallow Profiles 23

3.4 Trends 24

3.5 Do Templates Hold for Cluster Environments 26

4 Conclusions **28**

References **29**

Appendix **31**

List of Figures and Tables

Figure 1.1: High Saturation Hiding Pair of Galaxies 2

Figure 1.2: Schombert's Templates 3

Figure 1.3: Schombert's E and D Galaxies 5

Figure 2.1: Abell 1689 FITS 8

Figure 2.2: F814W Spectrum 10

Figure 2.3: Example Fit 13

Figure 2.4: Schombert's Templates 14

Figure 2.5: Example of Each Category of Fit 15

Figure 2.6: Cluster Radius Histograms (Individual Clusters) 16

Figure 2.7: Cluster Radius Histograms (Combined) 17

Figure 2.8: 16 kpc Magnitude Histograms (Individual Clusters) 18

Figure 2.9: 16 kpc Magnitude Histograms (Combined) 19

Table 1-4 Fragments: Each Galaxy's Data Sorted by Cluster 20

Table 5: Structural Data by Cluster 21

Figure 3.1: Cluster Radius Histograms (Combined) with KDE 23

Figure 3.2: 16 kpc Magnitude Histograms (Combined) with KDE 26

Table 1: Abell 209 31

Table 2: Abell 1423 33

Table 3: Abell 1689 35

Table 4: MACS J0416.1-2403 37

1 Introduction

1.1 Elliptical Structure

Out of all galaxy types, ellipticals Unlike the widely varying structure of spiral and irregular galaxies, elliptical galaxies are mostly homogeneous (Kormendy, 2015). Surface level differences, such as the disky and boxy classifications which define the shape of the elliptical, do not have much of an effect on the structural makeup of an elliptical. This can be seen especially well when looking at the surface brightness profiles of elliptical galaxies.

Surface density versus radius profiles are constructed by fitting ellipses starting from the center of a galaxy and moving outward taking into account the total luminosity, a measure of the light emitted, enclosed within each segment (Graham & Guzman, 2004). The magnitude, or brightness, derived from that luminosity is then plotted by radius. The resulting graph gives a good idea of the structural makeup of the galaxy. There are several fitting functions that can be used to approximate the profile at different sections, the most common nowadays being the Sersic fit and the historical $r^{1/4}$ variation of it (Graham & Driver, 2005).

When spirals are analyzed this way, the profiles are mostly unique from each other. The differing arm layouts and regions of high star-formation give each a distinct shape regardless of having the same size or magnitude. By contrast, it is difficult to differentiate between elliptical profiles of comparable magnitudes without plotting them together. Any anomalies can usually be identified by looking at an actual image of the galaxy in question, such as having a second galaxy close enough to be missed when looking at high saturation Flexible Image Transport System (FITS) image (Figure 1.1).

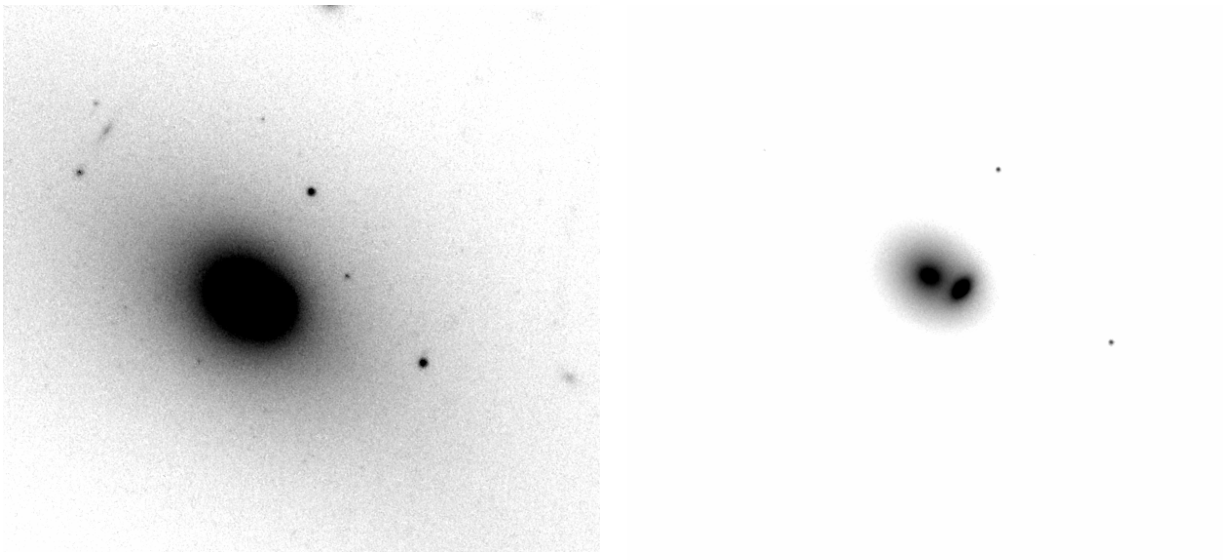

Figure 1.1: Example of a pair of galaxies that look like a single galaxy at high saturation.

1.2 Templates and Color Filters

The homogeneity of elliptical surface brightness profiles is such to the point that Schombert was able to develop a set of templates that match the majority of ellipticals, pictured in Figure 1.2 (Schombert, 2013). The templates range from absolute magnitude -21.5 to -25 and can be used to form templates for any luminosity within and a bit outside of that range. This range covers most galaxies but does omit those at the extremes.

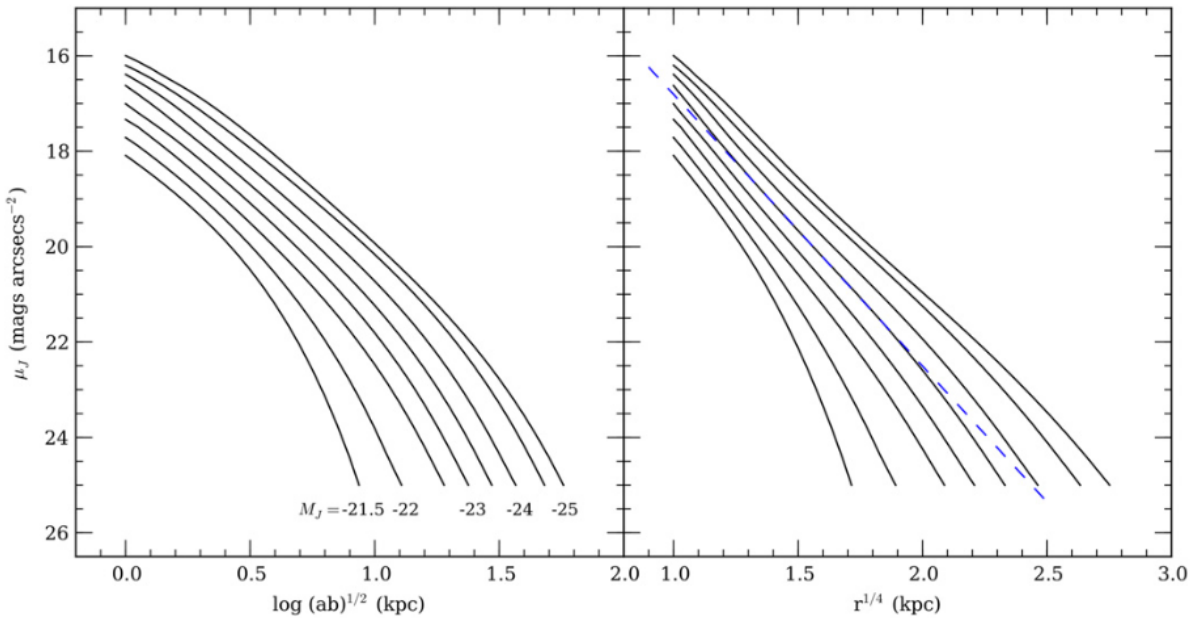

Figure 1.2: Templates developed by Schombert for elliptical galaxies (2015).

These templates were constructed using a set of 308 ellipticals in the near-infrared Johnson J color filter that match the traditional structure. Color filters limit the wavelengths of light that are absorbed by a detector. Since detectors only register the total light absorbed without any regard to wavelength, using a filter allows us to analyze and compare objects at specific wavelengths. For example, the Johnson J filter would not be useful for studying the prevalence of star formation, as it does not admit x-rays, which young stars produce in abundance.

This limited range also means that an object's magnitude does depend on the filter used to view it. Magnitudes are a value used to compare the brightness of objects. By doing so in different filters, we can draw conclusions about the makeup, age, and kinematics of different galaxies. A spiral galaxy would have a much higher magnitude in the x-ray region when compared to an elliptical, even if they shared a similar magnitude in other filters.

One issue with this is that due to redshift, the original wavelength of the light is not the same as that detected, so this is only possible with objects of similar redshift values. While the galaxies in my sample are at higher redshifts than those discussed in Section 1.3, the difference is not so great that any massive shift in wavelength will be present.

1.3 Anomalous Ellipticals

Schombert's templates are a good match for the majority of elliptical galaxies, both in the field and within clusters; however, he also noted that there is a subsection of ellipticals that do not match them. His survey identified that around 33% of the galaxies studied showed deviant behavior (Schombert 2015).

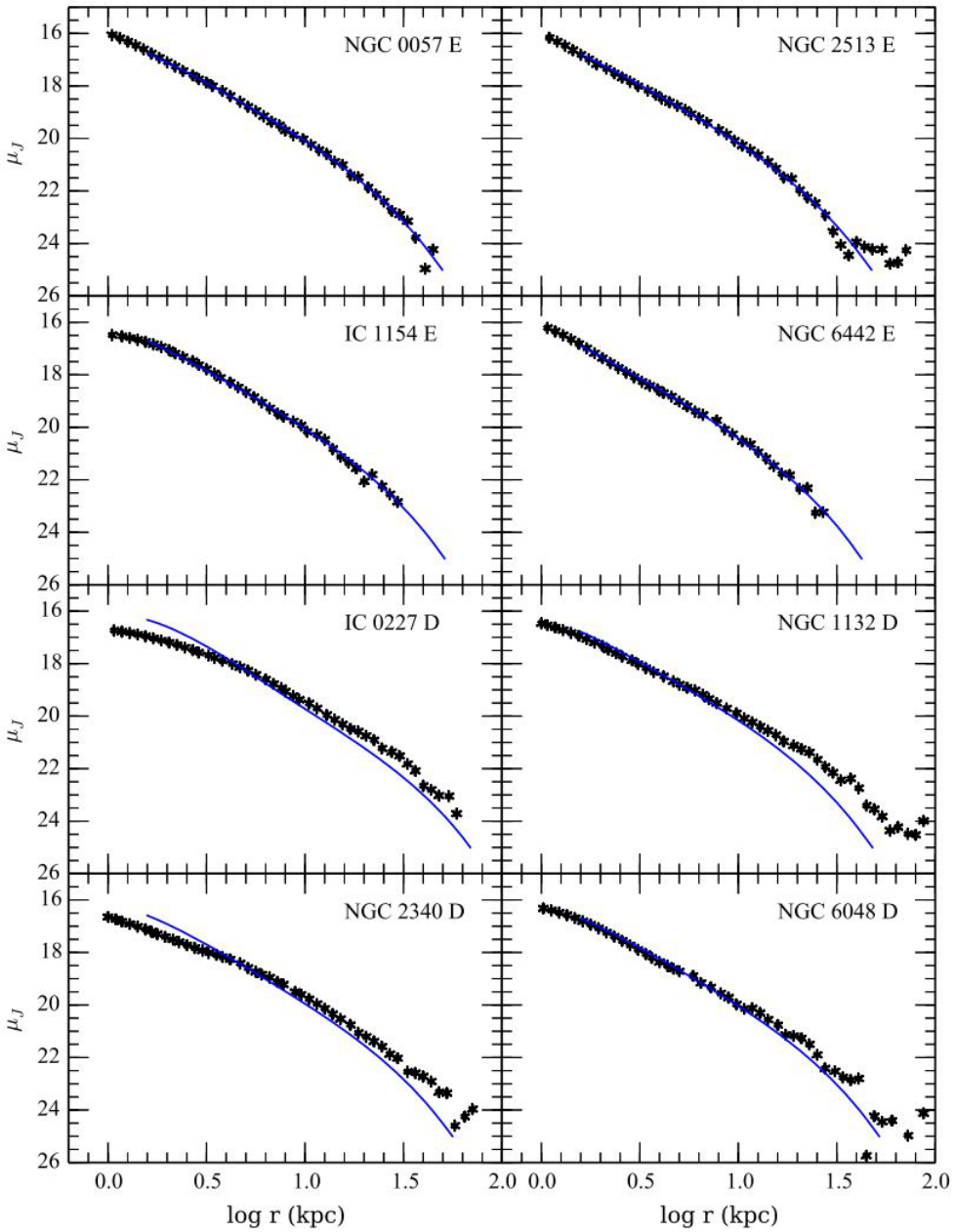

Figure 1.3: A selection of profiles from Schombert's initial detection (2015). Galaxies marked E are normal ellipticals and those marked D are the diffuse category.

Some profiles showed signs of recent interactions disrupting their luminosity distribution. Those only made up around 25% of the deviants, with the remaining 75% displaying similar deviations to each other. They vary with luminosity in a similar manner to typical ellipticals but have more extended surface brightness profiles. This indicates a more homogenous distribution

of mass through the galaxy, with classical ellipticals being more concentrated in the core region and less towards the edges. He has labeled these anomalous galaxies as D ellipticals, standing for diffuse (Figure 1.3). These D ellipticals are almost identical to their normal counterparts in every aspect except the structure, explaining why they had not been noticed until Schombert developed the templates.

1.4 Cluster Ellipticals

Schombert's study only involved field ellipticals. Galaxies in the field are mostly isolated and do not interact with other objects very often. Therefore, this research aims to uncover if this phenomenon is exhibited by ellipticals within clusters as well, which are closer and influence each other to a larger degree. Additionally, Schombert's sample was taken from low redshift in comparison to those in my sample. This means a significant amount of time has passed between the galaxies I have analyzed and his.

My initial predictions were that there would still be D ellipticals, but at a lower number than in the field, and that there would additionally be a selection of galaxies with steeper profiles. I also predicted that the more massive and denser a cluster is, the less common they will become. These predictions came from an expectation that in a cluster interactions between galaxies are significantly more common than in the field. Passing galaxies stripping mass from each other lead to proportionally denser cores with diffuse outer regions, making their surface brightness profiles steeper. After this kind of interaction, D elliptical profiles would start to look close to a typical elliptical, with typical ellipticals becoming steeper than the templates, which one would expect based on N-body simulations.

More dense clusters would naturally facilitate even more interactions, further decreasing the number of shallow profiles and boosting the quantity of steep profiles. We additionally

expect to see greater effects of tidal forces in denser clusters. This can take the form of the tidal truncation noted by Bothun and Schombert in bound populations (1988, 1990). Tidally truncated galaxies might fit the inner section of a template but begin to diverge in the outer reaches.

1.5 Mergers

An alternate possibility is that the profiles that don't fit are the product of galactic mergers. Disk galaxies colliding and merging is one potential method of elliptical formation (Naab, 2006). After merging, the structure of the new galaxy differs from that of other ellipticals, though they do eventually settle to the expected structure (Conselice, 2014). This temporary difference in structural makeup could lead to the divergence from the templates noted by Schombert (2015).

In a merger two or more galaxies of any type collide and merge into a single new galaxy almost always elliptical in shape due to the chaotic nature of the event. As the galaxies begin to merge, gas clouds within them collide, reigniting star formation. This is especially prominent in the central region of the newly formed galaxy, as that is where the most collisions occur. This would lead to my predicted steep profiles, with a denser core and a less dense outer region in comparison to similarly sized ellipticals.

Schombert also made a similar prediction. He theorized that the shallow profiles he found emerged from dry mergers (2015). Dry mergers consist of two or more gas deficient galaxies, almost always ellipticals. Due to the lack of gas, star formation is not reignited to nearly the same degree as a normal merger. The energy from the collision instead increases the kinetic energy of the objects in the galaxy, causing them to spread out. This leads to shallower profiles. Thus it's possible both shallow and steep profiles may result from different types of mergers.

2 Methods

2.1 Data Set and Acquisition

This project started with an overview of papers in order to locate galaxy clusters in our redshift range and color filter (Postman 2012). After compiling a suitably large selection we selected four clusters to focus on. The chosen clusters are Abell 209, Abell 1423, Abell 1689 (Figure 2.1), and MACS J0416 from the Cluster Lensing and Supernova survey with Hubble (CLASH). These four were selected due to having a large concentration of candidate galaxies and being sufficiently back in time to compare to the present-day galaxies used to develop Schombert's templates.

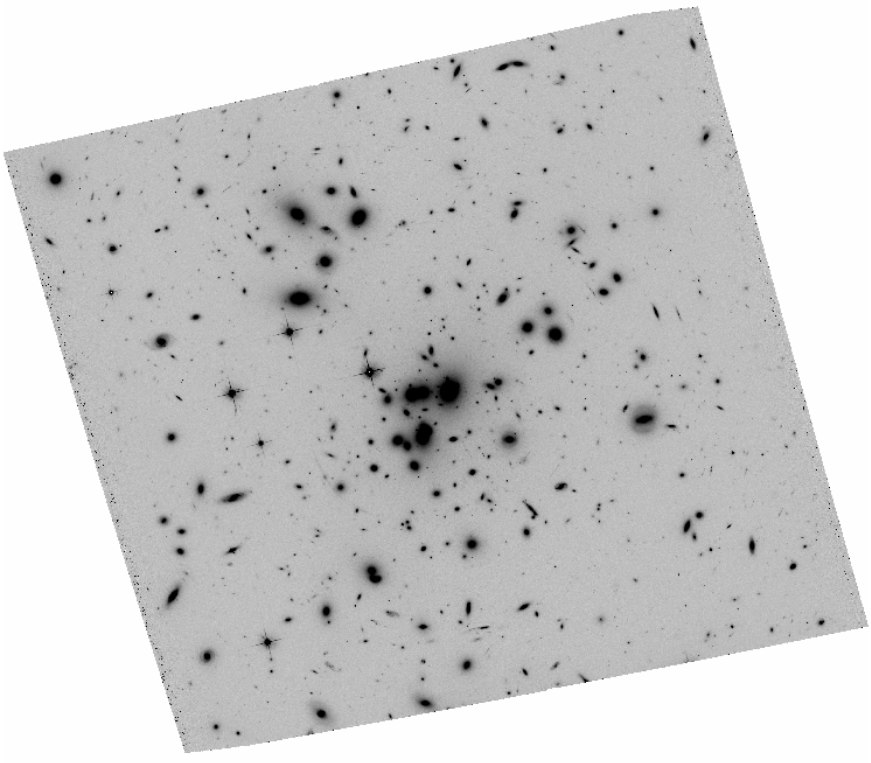

Figure 2.1: Abell 1689 FITS file image.

For each of the clusters we used NASA's Extragalactic Database (NED) to get several parameters, including the redshift of the cluster and its galactic extinction. Galactic extinction takes into account the absorption of light by objects such as gas and dust between the galaxy emitting the light and the observer, thus luminosity needs to be added to compensate. K-corrections are used to convert the data from the observer's frame into the equivalent from a rest frame of the object being observed, taking into account the redshift of an object.

Redshift itself is important, as clusters with too high or low redshifts are too far or not far enough backwards in cosmic time to provide an interesting comparison to Schombert's templates. The distance to the clusters, and thus their place in time, is derived by multiplying the redshift by the speed of light and dividing by the Hubble constant, 75 in our case. The Abell clusters lie in the $z = 0.18$ to 0.22 redshift range, just over 2 billion years in the past, with A1689 having a pixel to kpc conversion of 2.873 and A0209 and A1423 sharing a scale of 3.246. MACS J0416 has a redshift of $z = 0.397$, which converts to around 4 billion years and a pixel scale of 4.992 kpc per pixel.

The raw data for the four clusters came from the Mikulski Archive for Space Telescopes (MAST), a repository of astronomical data. We elected to use data from the Hubble Space Telescope archive, specifically the Advanced Camera for Surveys (ACS). Launched in 1990, the HST is a low Earth orbit satellite telescope. It has a primary mirror with a diameter of 2.4 meters and a secondary mirror with a diameter of 0.3 m. The ACS is a third-generation instrument that was installed in 2002 with a limiting magnitude of 27.0 Vega magnitudes. It had two main channels, the High-Resolution Channel (HRC) and the Wide Field Channel (WFC). In 2006, electronic failures led to both being temporarily offline. The WFC was restored in 2009, but the HRC was not. The data for our clusters was drawn from the WFC archives. Our selected data has

exposure times of 8080 seconds for A209, 8480 for A1423, 10740 for A1689, and 8074 for macs0416.

F814W was our chosen color filter due to its proximity to the 2MASS J color filter Schombert developed his templates with. F814W covers the range from approximately 700 to 950 nanometers, or the near-red range (Figure 2.2). This range is very similar to the Cousins I filter, which made converting into the necessary Johnson J filter a much easier task.

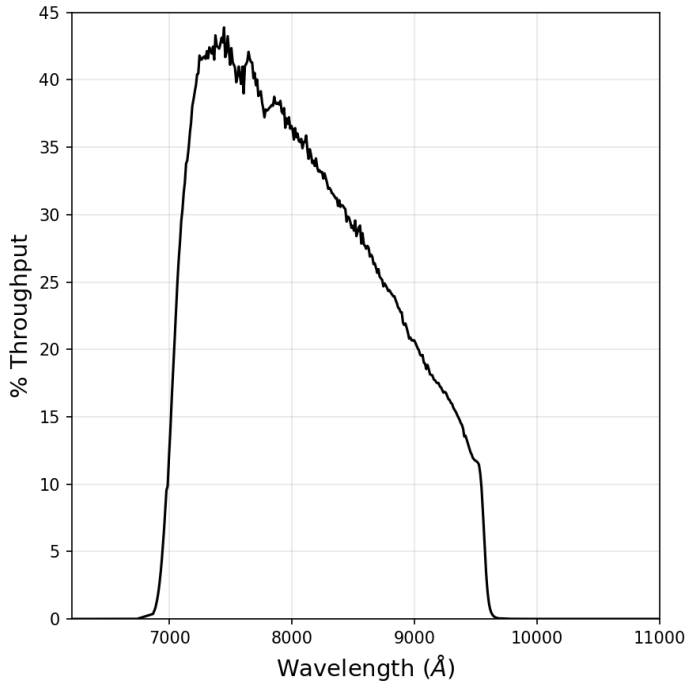

Figure 2.2: F814W WFC filter from the HST user documentation

2.2 Individual Galaxies

What we needed for the purpose of this research were the individual galaxies within the clusters. First it was necessary to identify which objects in the cluster fit our needs. This involved flagging every object with sufficient size and brightness in each of the FITS files and manually

deciding whether the object is an elliptical or not. There were also some that were too near other objects, and thus were not able to be analyzed.

After repeating this process for each cluster we had a total of 378 galaxies, 69 from Abell 0209, 87 from Abell 1423, 151 from Abell 1689, and 71 from MACS 0416. Abell 1689 was the first cluster we analyzed and had a less strict selection method for what galaxies would be good for this study, resulting in ellipticals too faint to be properly analyzed and even a couple non-ellipticals being included. More than two-thirds of the Abell 1689 galaxies were not usable in this study due to these issues. This experience helped refine our selection process for the other clusters, as we were more easily able to identify galaxies visually that would not work before plotting them. While some did still slip through, they were generally much closer to the galaxies that fit our criteria than those in Abell 1689.

Once the elliptical galaxies had been identified, the ARCHANGEL pipeline, developed by Schombert, went through the process of preliminary reduction (Schombert 2009). This was a recursive process of fitting ellipses to the galaxy, seeing how they fit the galaxy itself, removing any surrounding objects from the frame and re-fitting, removing the desired galaxy and just fitting the surrounding objects, removing that light and replotting the initial galaxy. The process is repeated until the ellipses properly fit the galaxy using a least squares scheme.

Once finished, the frame is converted by the ARCHANGEL pipeline into an XML format containing all the information needed to plot the galaxy. This includes the magnitude and radius for each point of the surface brightness profile, ellipse eccentricity, and several constants needed to properly correct the magnitude. These XML files are then passed on to me through a pickup site for plotting, fitting, and categorization.

2.3 Plotting and Fitting

I plotted the surface brightness profiles using a custom python program I have written. It takes the XML files passed to me by Schombert and extracts and cleans up all the needed data. Corrections and conversions are applied to the data. For the magnitudes of each ellipse, galactic extinction, cosmo sfb, and k-correction are all applied to each galaxy individually with universal conversions from the F814W color filter to the I filter and then to J in order to match the templates with a final Vega-magnitude correction applied. For the radius, sqrt(a*b), and ellipse eccentricity are used to get a more accurate value which is then converted from arcseconds to kiloparsecs using the cluster specific conversion factor.

For the purposes of plotting I used the matplotlib.pyplot library. I wrote a Sersic function in order to calculate both $r^{1/n}$ and $r^{1/4}$ fits for the profiles, with the latter being the default plotted. For the purposes of analysis, the magnitude scale is inverted and the radius is plotted in $kpc^{1/4}$, with logarithmic scaling used for published results. Both the galaxy's data and Sersic profile are plotted on the same graph (Figure 2.3).

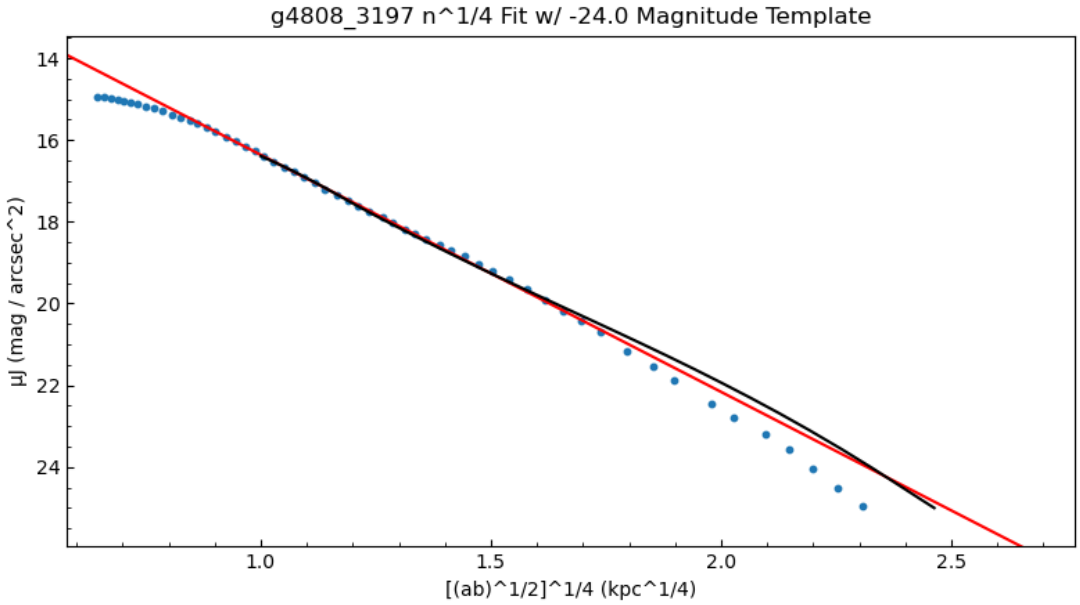

Figure 2.3: Example of a fit. The blue dots represent the galaxy data, the red line is the $n^{1/4}$ fit, and the black is the template fit discussed in X.4.

2.4 Templates and Categorization

This script also builds a template based on the 16 kiloparsec magnitude, a measure of the magnitude 16 kiloparsecs from the center of the galaxy, and the set of elliptical templates developed by Schombert (Figure 2.4). This is then plotted on top of the graph of the galaxy. In almost every case, the 16 kiloparsec magnitude provides only a rough match, requiring manual tweaking of the magnitude in order to match the profile. Once properly calibrated, or as close as possible, the profile is saved.

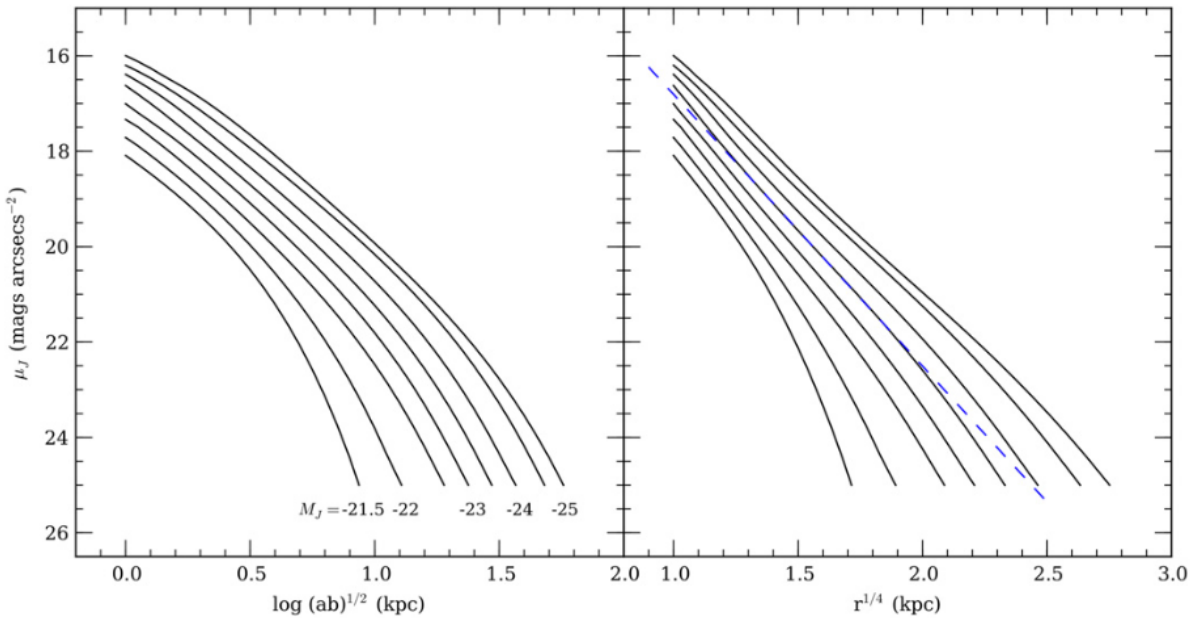

Figure 2.4: Templates developed by Schombert for elliptical galaxies (2015).

Unfortunately, Schombert's templates only cover magnitude ranges from -21.5 to -25, which covers most, but not all galaxies. Any galaxies that fall too far outside that range, for this study below -21 and above -25, are not useful for this application. Those that do fall within this section are sorted by cluster and then split into magnitude sections (i.e. -22 to -23). Further sorting is done by how well the profile fits the template. Sorting is performed manually by looking at the profile and determining what category (good, steep, shallow, or weird) it falls under.

Most galaxies are good fits to their related template, but not all. Steep fits are galaxies with profiles steeper than their closest profile predicts, indicating a more compact galaxy than expected. Shallow fits are the opposite, with shallower profiles that indicate more diffuse galaxies. There are also a few profiles that do not fall under any category and are thus labeled as weird fits; these display no consistency in their deviations, indicating they result from unique

and/or very recent interactions. Examples of what the four fit categories look like can be seen in Figure 2.5.

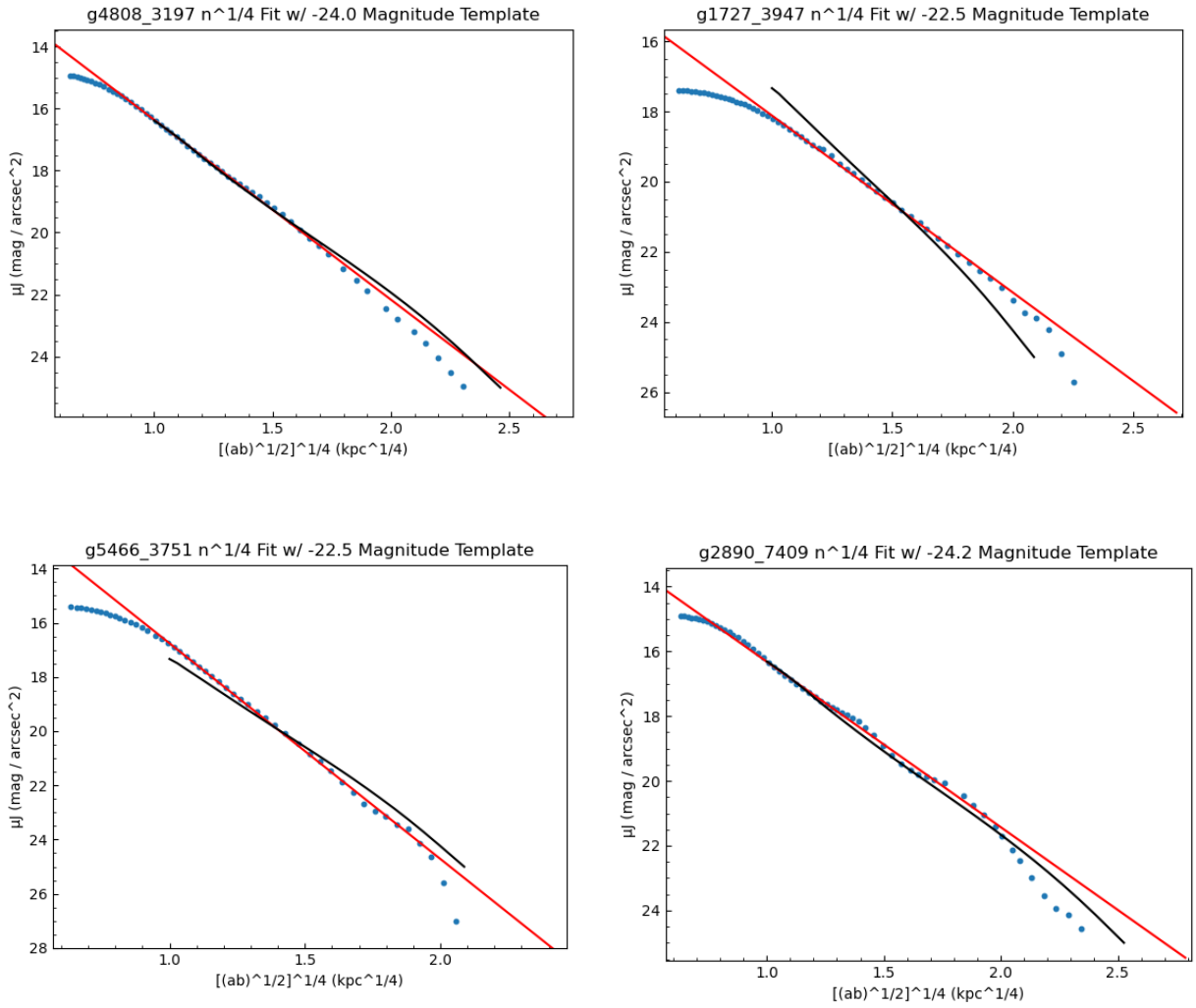

Figure 2.5: Examples of a good (top left), shallow (top right), steep (bottom left), and weird (bottom right) profile fits when compared to their respective template.

Once sorted, all four categories are plotted in histograms by both 16 kiloparsec magnitude and radius in cluster. Radius was determined by designating the most prominent object in the FITS image as the center of the cluster, or in between if more than one stood out,

and using the Pythagorean identity to find the distance to the current galaxy. This value is then converted to kiloparsecs using the scale factor at the cluster's redshift and finally put into log scale to produce more readable graphs. The clusters are plotted both individually and collectively (Figure 2.6-9). Tables 1-4 list the galaxies along with their profile type, 16 kiloparsec magnitude, and log of their radius in the cluster in kiloparsecs.

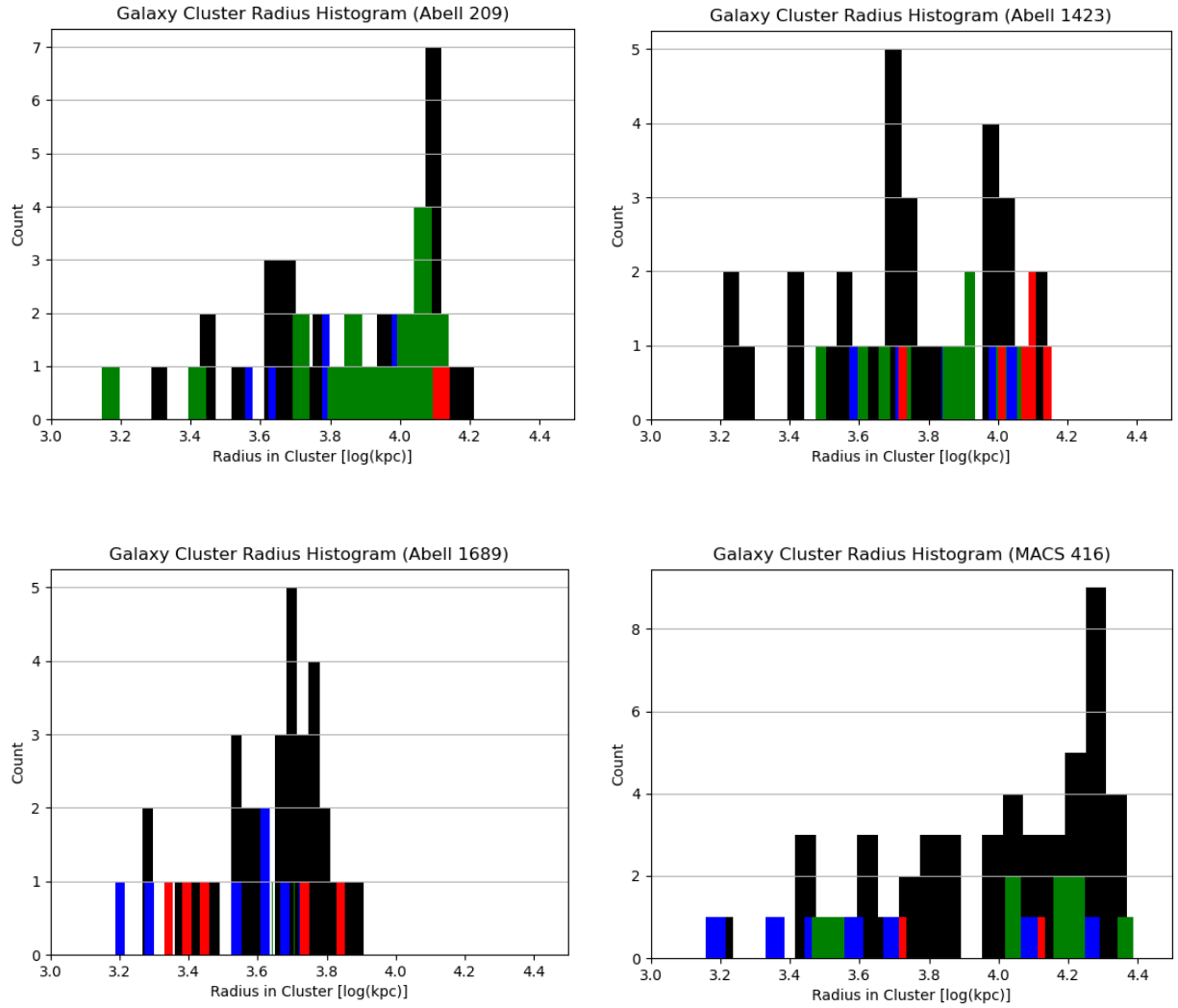

Figure 2.6: Histograms of the clusters by their radius in the cluster (log(kpc)). Black represents good fits, green shallow, blue steep, and red weird.

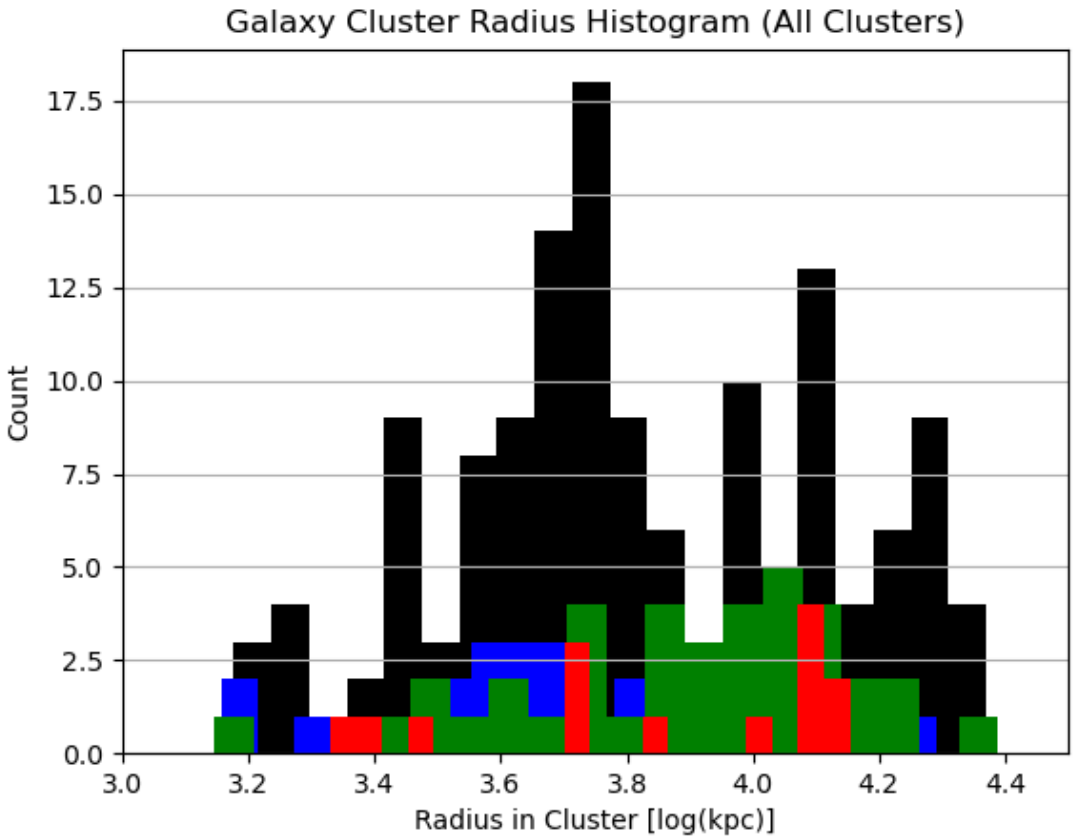

Figure 2.7: Combined histogram of all the clusters by radius in cluster. Black represents good fits, green shallow, blue steep, and red weird.

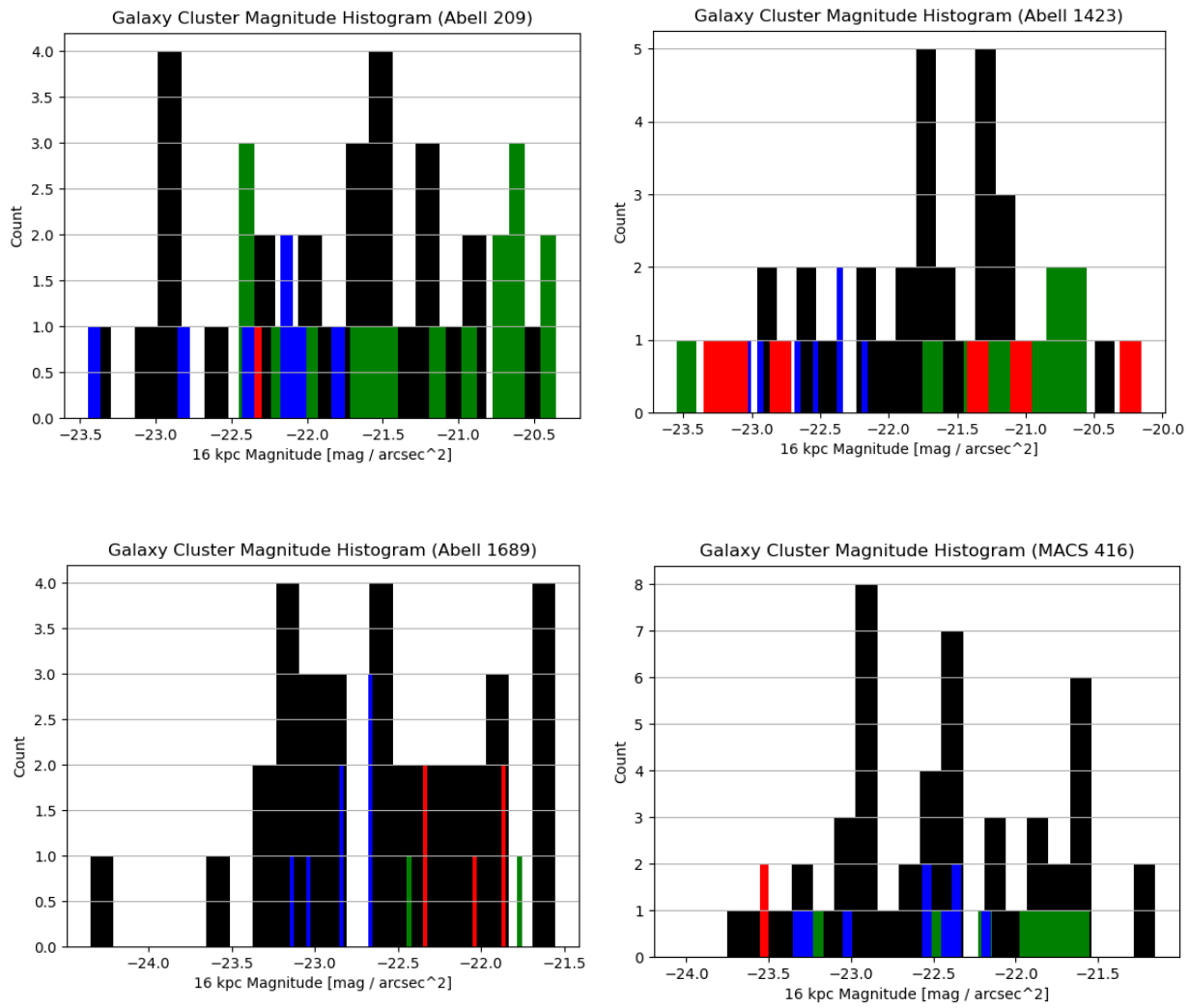

Figure 2.8: Histograms of the clusters by their 16 kpc magnitude (mag/arcsec^2). Black represents good fits, green shallow, blue steep, and red weird.

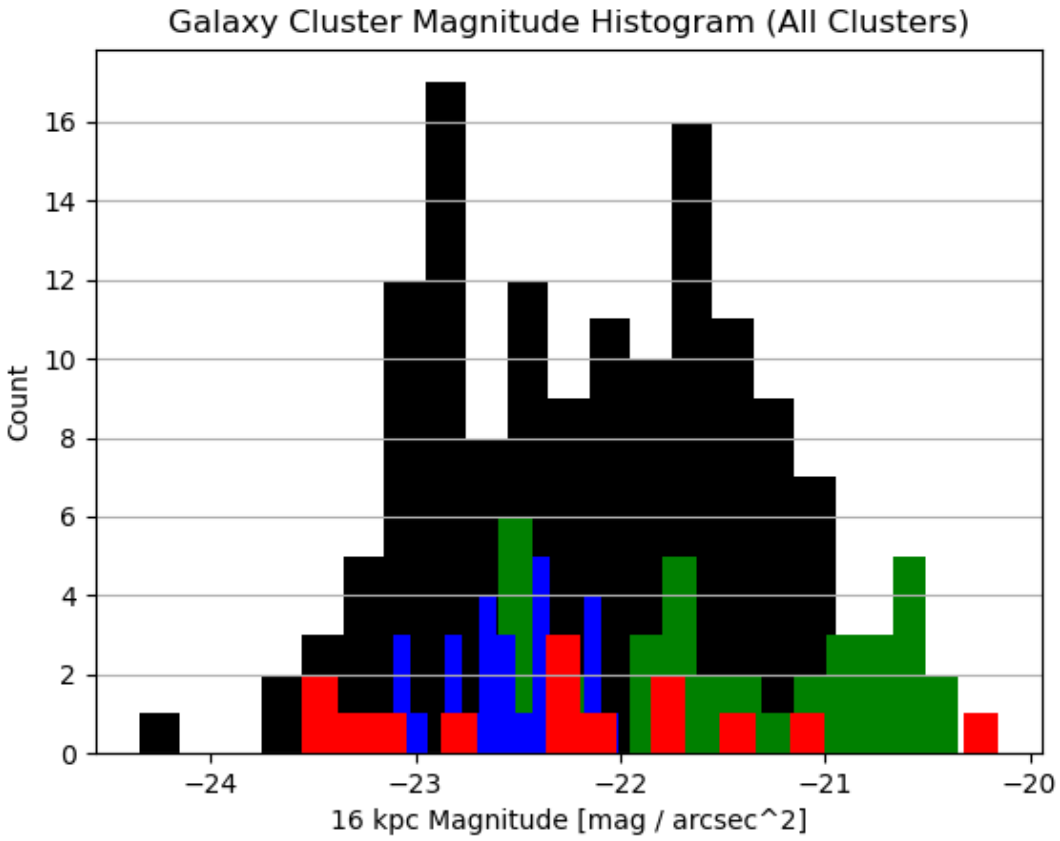

Figure 2.9: Combined histogram of all the clusters by 16 kpc magnitude. Black represents good fits, green shallow, blue steep, and red weird.

First few lines of Tables 1-4 (See Appendix for the rest of these tables)

Table 1. Abell 209

Galaxy	profile type	log R_c (kpc)	M_{16kpc} (J mags)
g0796_7755	d	4.21	−22.85
g2008_2203	d	4.12	−21.95
g2481_4893	d	3.91	−21.15
g2630_1914	d	4.10	−21.65
g2641_2062	d	4.09	−22.95

Table 2. Abell 1423

Galaxy	profile type	log R_c (kpc)	M_{16kpc} (J mags)
g2542_8115	d	4.11	−22.15
g2544_6769	d	3.99	−22.05
g3394_4216	d	3.76	−21.75
g3814_8001	d	4.02	−21.15
g3919_6182	d	3.72	−21.75

Table 3. Abell 1689

Galaxy	profile type	log R_c (kpc)	M_{16kpc} (J mags)
g0932_3225	d	3.75	−21.85
g1022_1789	d	3.75	−22.35
g1071_2320	d	3.70	−22.85
g1082_1310	d	3.79	−23.65
g1136_1720	d	3.73	−22.15

Table 4. MACS J0416.1-2403

Galaxy	profile type	log R_c (kpc)	M_{16kpc} (J mags)
g1491_6966	d	4.24	−22.85
g2727_6460	d	4.02	−22.75
g2769_8382	d	4.23	−22.35
g3161_2183	d	4.27	−22.15
g3214_2132	d	4.27	−22.15

(d represents a good fit, u a shallow fit, o a steep fit, and w a weird fit)

3 Discussion

3.1 Results

Table 5: Structural Data by Cluster

Mag Block	21-22	22-23	23-24	24-25	All	Percentage
Abell 209						
Total	20	21	11	2	54	
Good Fit	10	11	6	1	28	51.9
Shallow Fit	10	4	4	0	18	33.3
Steep Fit	0	5	1	1	7	13.0
Weird Fit	0	1	0	0	1	1.85
Abell 1423						
Total	21	20	7	6	54	
Good Fit	10	15	3	2	30	55.6
Shallow Fit	8	0	0	2	10	18.5
Steep Fit	0	5	3	0	8	14.8
Weird Fit	3	0	1	2	6	11.1
Abell 1689						
Total	20	21	5	1	47	
Good Fit	13	14	5	1	33	70.2
Shallow Fit	1	1	0	0	2	4.26
Steep Fit	1	6	0	0	7	14.9
Weird Fit	5	0	0	0	5	10.6
MACS0416						
Total	5	27	27	9	68	
Good Fit	4	17	21	6	48	70.6
Shallow Fit	1	4	3	1	9	13.2
Steep Fit	0	6	3	0	9	13.2
Weird Fit	0	0	0	2	2	2.94

Table 5 *(continued)*

Mag Block	21-22	22-23	23-24	24-25	All	Percentage
All Clusters						
Total	66	89	50	18	223	
Good Fit	37	57	35	10	139	62.3
Shallow Fit	20	9	7	3	39	17.5
Steep Fit	1	22	7	1	31	13.9
Weird Fit	8	1	1	4	14	6.28

After analyzing our four clusters (compiled into Table 5), the percentage of galaxies that do not fit the templates does not vary too much from the 33% figure Schombert (2015) found. Overall 37% of the galaxies did not fit with their closest template. When removing the weird profiles from the total, we find that around 33% of our galaxies do not match with the templates, which is remarkably close to the concentration in the field. However, it is split between shallow, 18.6% and steep, 14.8%, profiles, as opposed to the purely shallow profiles in the field sample.

MACS0416 and Abell 1423 have a similar split between shallow and steep profiles with the concentrations of each being close to equal. Abell 209 and 1689 by contrast have significant differences. Abell 209 has a much larger percentage of shallow profiles while Abell 1689 has almost none. This may be due to differences in the density of each cluster, with Abell 1689 being much richer. Cluster density potentially plays a role in the formation and destruction of shallow profile ellipticals, as increased richness leads to an increased number of interactions between galaxies. What is interesting to note is that the percentage of steep profiles is consistent across all the clusters.

3.2 Merger Formation and Steep Profiles

One potential method of elliptical galaxy formation is through galaxy mergers. When two galaxies get close enough, they will begin to merge. Based on N-body simulations, this process leads to the formation of elliptical galaxies, regardless of the class of the original galaxies (Moore 1998). Mergers also lead to an at least temporarily denser and brighter core region of the new galaxy, as the energy of the collision ignites star formation and the new stellar mass converges into the center of the galaxy. A brighter than normal core is what leads to a steeper profile, so it seems plausible that recent galaxy mergers result in the steeper profiles detected in my research.

This also explains why we see steep profiles when looking at cluster environments and not in the field, as interactions between galaxies are significantly more common in a cluster than outside of one. Mergers being uncommon in the field means that steep profiles would also be rare to find. Not only would a merger need to occur, but it would need to have been recent enough to have not evolved away from the dense core stage. The new galaxy will eventually settle into what we consider a typical elliptical structure as the increased kinetic energy from star formation redistributes and begins to expand the galaxy.

3.3 Shallow Profiles

Heating is also potentially responsible for the shallow profiles existence as well. As the galaxy increases in kinetic energy, it may become more diffuse than a normal elliptical. This leads to a shallower profile. Galaxies may be heated to this point by the additional star formation from a merger, indicating that shallow profiles may be evidence of previous mergers. It could also be the case that the increased kinetic energy is due to tidal heating as the galaxy moves

through potential fields. In this case we would expect to see shallow profiles display extended orbits through the cluster, and that is what I found.

3.4 Trends

There is a slight trend in the shallow profiles towards the outer reaches of the clusters (Figure 3.1). This indicates that they have extended orbits that take them deeper into the cluster's potential well. The increase in energy from descending into the potential well causes them to expand. Another cause for this trend may be that the outer sections of a cluster are less dense, and thus the shallow ellipticals would interact less and keep their form longer.

By contrast, the steep profiles match the normal ellipticals almost perfectly (Figure 1). This further strengthens my theory that they come from mergers. As the number of normal ellipticals increases, the number of recently merged ellipticals should also increase. Another trend with steep profiles is that they tend to have higher 16 kpc magnitudes (Figure 3.2). This makes sense, as the denser core leads to more luminosity being enclosed in that range than would be expected for a galaxy that size.

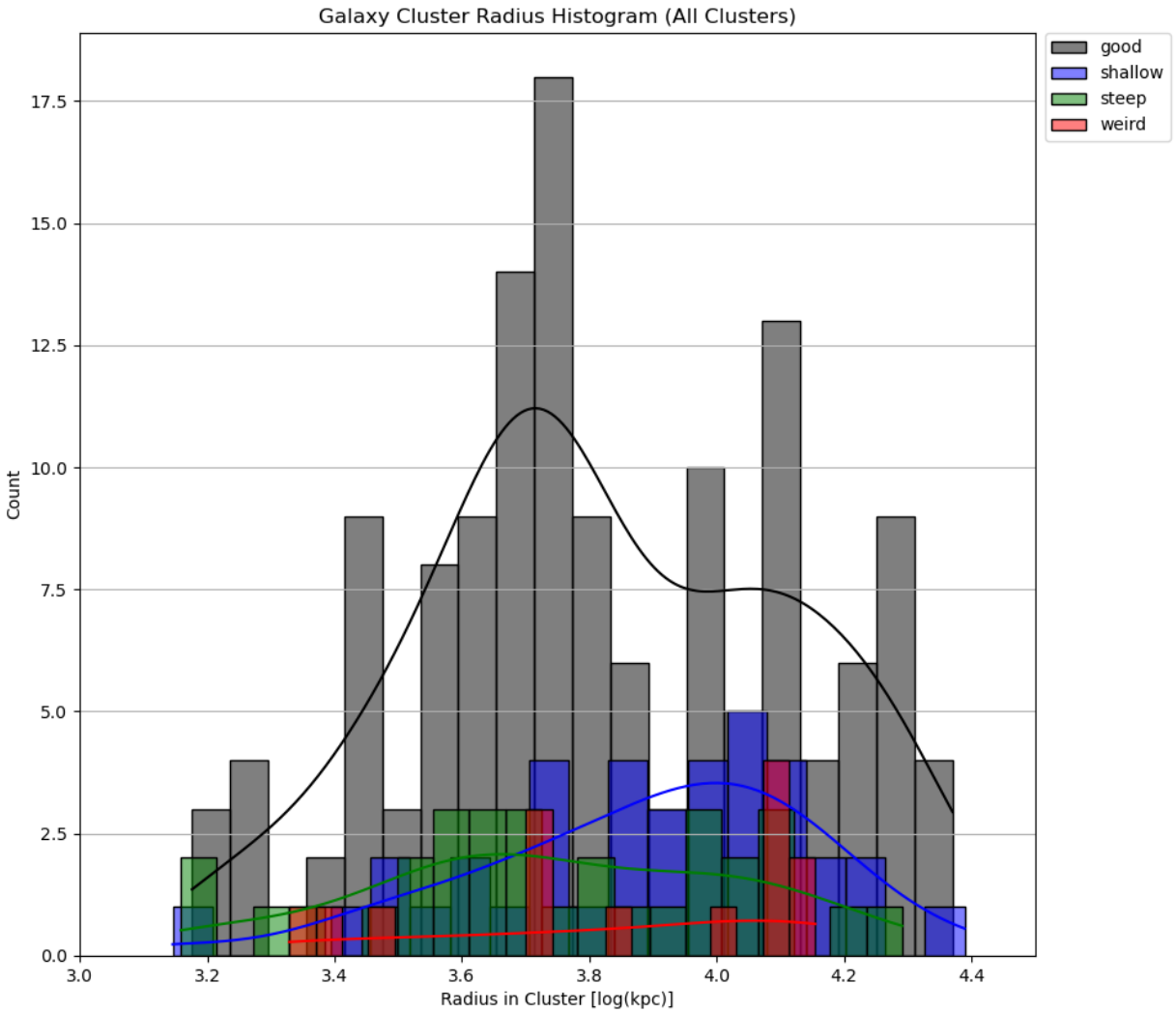

Figure 3.1: Combined histogram of all the clusters by radius in cluster with the addition of a kernel density estimation line to show trends.

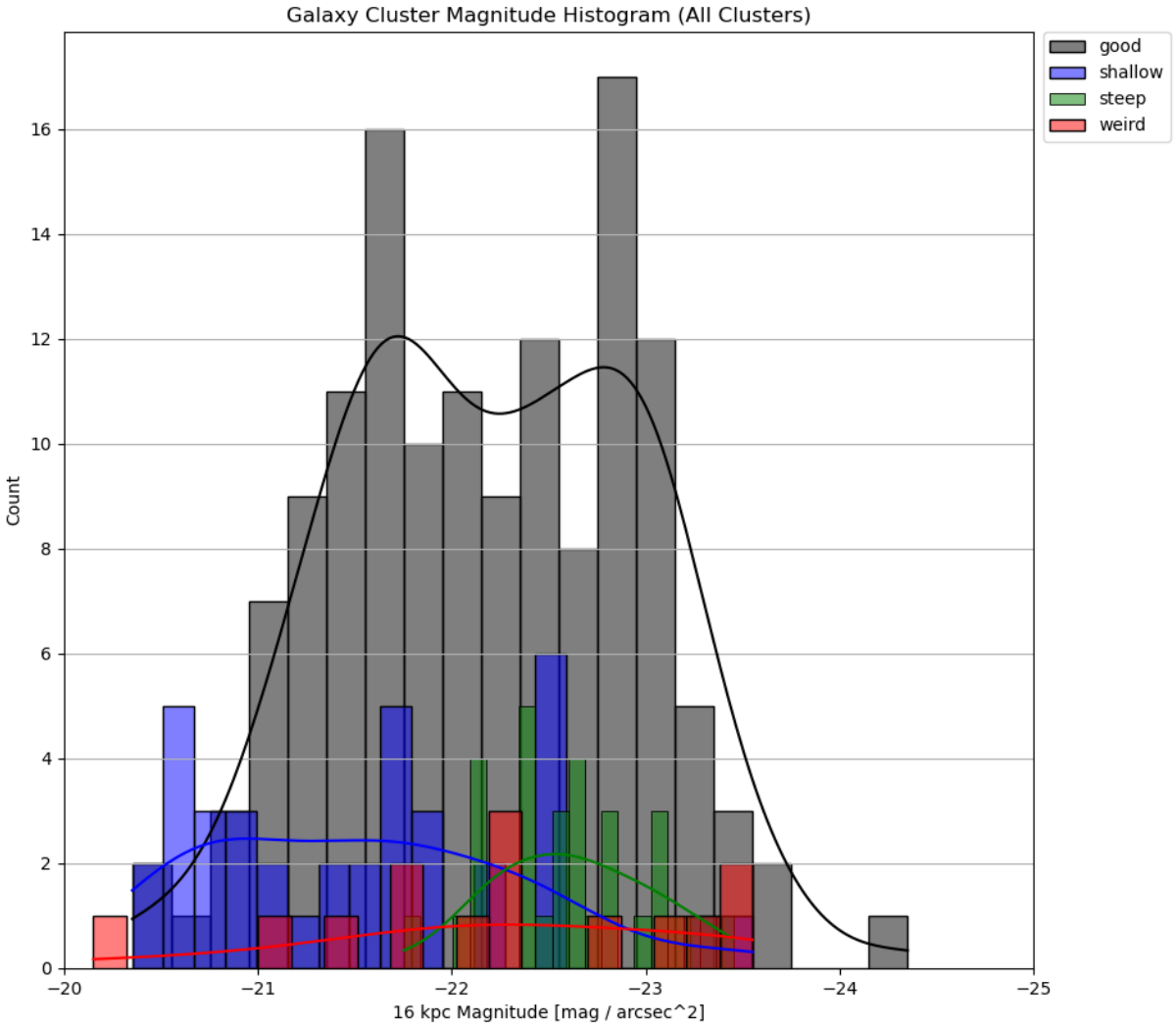

Figure 3.2: Combined histogram of all the clusters by 16 kpc magnitude with the addition of a kernel density estimation line to show trends.

3.5 Do Templates Hold for Cluster Environments

Schombert's templates were built using field galaxies (2015). Within the field they work very well, with galaxies that do not match following a distinct pattern of structural difference. However, they may not be quite so well suited for cluster environments. While more than half of the galaxies do still fit the templates well, many of them show signs of tidal truncation. Additionally, the split between shallow, steep, and weird profiles in the remaining galaxies is a

less concrete trend. This is especially true as it varies from cluster to cluster. The templates may simply not be suited for the more chaotic environment of a cluster.

Despite this, I hold that these templates are still useful for cluster research. Most galaxies fit the templates, even if just in the central regions. By comparing the outer reaches of the galaxy to the core-fit template, one can make guesses as to previous interactions the galaxy has experienced. Using templates, tidally truncated galaxies are easy to identify. So while they may not be able to predict the shape of galaxies quite as well in a cluster, Schombert's templates are an analytical tool worth considering.

4 Conclusions

From this study I have concluded there are not just two structural families of elliptical galaxies, but three. The shallow and steep profile galaxies display enough unique qualities to be categorized separately from traditional ellipticals. Steep profiles seem to be the result of galaxy mergers. Shallow profiles may also come from mergers but are more likely due to increased kinetic energy from interactions with the cluster's potential well. Whether these are simply temporary states that eventually lead to a standard elliptical structure requires further research.

Looking at even more distant clusters would be a good place to start. Creating a timeline of shallow and steep profile concentration as the universe evolves could provide a window into elliptical development and formation. With the launch of the James Webb Space Telescope the depth we can look back is greater than ever, so the time seems right to begin working on this. The JWST also would provide an opportunity to look at clusters in different wavelengths, as it covers the mid-infrared range.

In the short term, Schombert and I may perform this same analysis on the rest of the CLASH sample, which was cut from the initial survey due to time-constraints. Elliptical structure within clusters is a surprisingly untapped field of study, and one I would very much like to see expanded. They may not look as flashy as their spiral cousins, but their structure and formation can tell us a lot about the validity of dark matter models and how the early universe developed into the structures we observe today, for which I hope my research serves as a foundation.

Appendix: Continued Tables 1-4

Table 1. Abell 209

Galaxy	profile type	log R_c (kpc)	M_{16kpc} (J mags)
g0796_7755	d	4.21	−22.85
g2008_2203	d	4.12	−21.95
g2481_4893	d	3.91	−21.15
g2630_1914	d	4.10	−21.65
g2641_2062	d	4.09	−22.95
g2664_5254	d	3.88	−21.55
g2875_6614	d	3.94	−21.35
g3113_3742	d	3.87	−21.85
g3467_3685	d	3.82	−20.95
g3710_4423	d	3.66	−22.95
g3737_4194	d	3.69	−22.95
g3990_4209	d	3.62	−21.45
g4005_5484	d	3.56	−21.55
g4435_6207	d	3.64	−20.85
g4808_3197	d	3.77	−23.05
g5346_1329	d	4.08	−22.25
g5351_4519	d	3.29	−22.05
g5603_3767	d	3.65	−21.55
g5608_5638	d	3.46	−21.65
g5704_5423	d	3.43	−21.05
g5800_6205	d	3.67	−23.45
g5891_1423	d	4.08	−21.25
g6023_1138	d	4.11	−22.55
g6300_5955	d	3.72	−22.25
g6564_1382	d	4.11	−20.65
g6888_4796	d	3.79	−21.25
g7110_1929	d	4.08	−21.65
g7763_5173	d	3.95	−20.35
g0832_4150	u	4.14	−20.75
g1017_4344	u	4.12	−22.15

Table 1 *(continued)*

Galaxy	profile type	log R_c (kpc)	M_{16kpc} (J mags)
g1721_3542	u	4.07	−20.95
g1727_3947	u	4.05	−21.45
g2005_4512	u	3.99	−20.75
g2861_5355	u	3.85	−20.65
g4753_6620	u	3.73	−20.65
g4994_5431	u	3.15	−22.45
g5655_6568	u	3.74	−20.45
g5756_4695	u	3.42	−22.45
g6443_3617	u	3.81	−20.35
g6502_6849	u	3.89	−21.55
g6615_3174	u	3.90	−22.45
g6988_2900	u	3.97	−21.95
g7360_6896	u	3.99	−21.15
g7568_7292	u	4.05	−21.65
g8359_6672	u	4.09	−20.65
g3649_2937	o	3.90	−21.75
g4351_5897	o	3.56	−23.45
g5466_3751	o	3.64	−22.15
g6409_7626	o	3.99	−22.85
g6533_6116	o	3.79	−22.05
g6853_5509	o	3.80	−22.35
g7925_5954	o	4.00	−22.15
g1323_3936	w	4.09	−22.35

Table 2. Abell 1423

Galaxy	profile type	log R_c (kpc)	M_{16kpc} (J mags)
g2542_8115	d	4.11	−22.15
g2544_6769	d	3.99	−22.05
g3394_4216	d	3.76	−21.75
g3814_8001	d	4.02	−21.15
g3919_6182	d	3.72	−21.75
g3923_4719	d	3.56	−21.85
g4253_4637	d	3.43	−22.95
g4273_6149	d	3.64	−21.15
g4381_3517	d	3.72	−22.95
g4454_3997	d	3.57	−22.65
g4621_4073	d	3.51	−21.35
g4934_4476	d	3.23	−21.25
g5073_5491	d	3.21	−22.65
g5111_5586	d	3.29	−21.75
g5191_4174	d	3.44	−21.75
g5288_1871	d	4.01	−21.15
g5515_3939	d	3.58	−21.75
g6228_5973	d	3.71	−21.65
g6291_5767	d	3.69	−22.45
g6331_4330	d	3.68	−23.25
g6647_5764	d	3.77	−21.05
g6672_2659	d	3.97	−20.35
g6698_5389	d	3.75	−21.35
g6756_4911	d	3.76	−20.85
g7019_5464	d	3.83	−21.55
g7068_2625	d	4.01	−21.85
g7442_1475	d	4.14	−21.45
g7466_6356	d	3.96	−22.15
g7749_2504	d	4.08	−21.35
g7850_5679	d	3.98	−21.35

Table 2 *(continued)*

Galaxy	profile type	log R_c (kpc)	M_{16kpc} (J mags)
g2568_5409	u	3.90	−20.65
g3105_6416	u	3.89	−21.15
g3317_3513	u	3.86	−20.75
g3993_7311	u	3.91	−20.85
g4121_3517	u	3.75	−21.25
g5113_6279	u	3.62	−20.55
g5916_4970	u	3.47	−23.55
g6028_2010	u	4.01	−21.35
g6384_4507	u	3.68	−21.65
g7510_2189	u	4.09	−20.95
g1739_7214	o	4.11	−22.15
g2345_6891	o	4.02	−22.65
g2379_7555	o	4.07	−22.35
g2412_2777	o	4.04	−22.75
g3914_6947	o	3.86	−23.05
g5300_6106	o	3.57	−22.55
g6576_5033	o	3.71	−22.95
g7294_3057	o	3.99	−22.35
g1500_2338	w	4.15	−22.85
g2738_8263	w	4.11	−23.15
g2890_7409	w	4.02	−23.35
g3564_1613	w	4.08	−20.15
g5905_3684	w	3.71	−21.05
g7285_1761	w	4.11	−21.35

Table 3. Abell 1689

Galaxy	profile type	log R_c (kpc)	M_{16kpc} (J mags)
g0932_3225	d	3.75	−21.85
g1022_1789	d	3.75	−22.35
g1071_2320	d	3.70	−22.85
g1082_1310	d	3.79	−23.65
g1136_1720	d	3.73	−22.15
g1226_3085	d	3.68	−22.25
g1255_3883	d	3.76	−22.65
g1354_0476	d	3.87	−21.65
g1690_3515	d	3.62	−22.65
g1814_1158	d	3.70	−21.55
g2026_0559	d	3.80	−23.25
g2056_1212	d	3.66	−23.15
g2147_2001	d	3.41	−22.45
g2149_4076	d	3.67	−21.55
g2264_3718	d	3.55	−24.35
g2360_2123	d	3.27	−22.95
g2687_0627	d	3.75	−23.15
g2759_1961	d	3.26	−22.55
g2853_3766	d	3.53	−21.65
g2894_4041	d	3.62	−22.85
g2951_0869	d	3.70	−23.05
g2984_1639	d	3.45	−23.35
g3254_3742	d	3.55	−23.15
g3332_1716	d	3.47	−22.45
g3468_3124	d	3.39	−23.05
g3544_4271	d	3.72	−21.95
g3732_4297	d	3.75	−21.85
g3749_3415	d	3.56	−22.05
g3907_3335	d	3.58	−23.05
g4353_1753	d	3.71	−23.15

Table 3 *(continued)*

Galaxy	profile type	log R_c (kpc)	M_{16kpc} (J mags)
g4431_1824	d	3.72	−22.65
g4472_4232	d	3.83	−22.35
g5211_1143	d	3.91	−22.05
g3890_3666	u	3.64	−21.75
g4152_3753	u	3.71	−22.45
g1128_1593	o	3.75	−22.65
g1257_1990	o	3.68	−23.05
g2672_1113	o	3.63	−22.85
g2702_3255	o	3.28	−22.85
g2986_2097	o	3.19	−22.65
g3315_1240	o	3.62	−22.65
g3822_3244	o	3.54	−23.15
g2675_1611	w	3.46	−22.35
g2890_1863	w	3.33	−21.85
g2964_3435	w	3.39	−22.05
g3322_0825	w	3.73	−21.85
g5027_1497	w	3.85	−22.35

Table 4. MACS J0416.1-2403

Galaxy	profile type	log R_c (kpc)	M_{16kpc} (J mags)
g1491_6966	d	4.24	−22.85
g2727_6460	d	4.02	−22.75
g2769_8382	d	4.23	−22.35
g3161_2183	d	4.27	−22.15
g3214_2132	d	4.27	−22.15
g3243_8217	d	4.17	−22.85
g3322_6829	d	3.96	−22.35
g3488_5880	d	3.78	−22.95
g3488_5945	d	3.79	−22.35
g3506_5807	d	3.77	−23.15
g3571_1997	d	4.27	−21.55
g3746_5646	d	3.66	−22.85
g4026_4259	d	3.87	−22.95
g4079_2980	d	4.12	−22.95
g4130_6226	d	3.62	−21.75
g4139_4929	d	3.62	−22.45
g4167_5385	d	3.42	−23.25
g4431_5783	d	3.18	−23.55
g4505_7888	d	4.06	−22.55
g4517_4469	d	3.75	−23.35
g4604_6245	d	3.52	−22.45
g4670_7730	d	4.03	−22.55
g4679_2437	d	4.20	−22.05
g5161_5404	d	3.43	−21.75
g5236_5502	d	3.46	−21.85
g5290_6870	d	3.85	−23.05
g5312_2598	d	4.18	−22.55
g5334_5044	d	3.64	−22.15
g5423_7562	d	4.02	−22.95
g5491_4284	d	3.89	−22.55

Table 4 *(continued)*

Galaxy	profile type	log R_c (kpc)	M_{16kpc} (J mags)
g5723_5020	d	3.78	−22.65
g5797_2669	d	4.19	−22.35
g6056_7887	d	4.13	−21.55
g6383_4980	d	3.96	−21.55
g6391_3461	d	4.14	−21.25
g6412_3010	d	4.19	−23.45
g6422_1236	d	4.37	−21.65
g6445_2392	d	4.26	−23.05
g6537_4892	d	4.00	−21.85
g6616_2404	d	4.27	−22.65
g6648_2191	d	4.29	−21.85
g6706_1808	d	4.33	−22.45
g6722_2156	d	4.30	−21.65
g6984_2798	d	4.26	−21.15
g6985_5042	d	4.08	−23.05
g7197_1917	d	4.35	−23.75
g7206_1773	d	4.36	−22.85
g7214_2715	d	4.28	−21.65
g2058_3979	u	4.18	−22.55
g4000_5765	u	3.53	−21.95
g4031_2412	u	4.21	−21.75
g4794_5022	u	3.46	−21.55
g5283_3447	u	4.05	−22.15
g5573_3683	u	4.02	−23.25
g6341_2916	u	4.20	−22.45
g6507_2945	u	4.21	−21.85
g7502_1589	u	4.39	−21.65
g3267_3504	o	4.10	−22.15
g3874_6237	o	3.71	−23.35
g3915_5644	o	3.57	−22.45
g4165_6104	o	3.55	−23.05
g4945_5548	o	3.16	−22.35

Table 4 *(continued)*

Galaxy	profile type	log R_c (kpc)	M_{16kpc} (J mags)
g5022_5101	o	3.48	−23.25
g5091_5684	o	3.34	−22.55
g7197_2609	o	4.29	−22.55
g7904_5987	o	4.21	−22.35
g2884_3527	w	4.13	−23.55
g3910_4871	w	3.71	−23.55

References

Bender, R., Kormendy, J., Cornell, M. E., and Fisher, D. B., "Structure and Formation of cD Galaxies: NGC 6166 in ABELL 2199", *The Astrophysical Journal*, vol. 807, no. 1, 2015. doi:10.1088/0004-637X/807/1/56.

Bothun, G. D. and Schombert, J. M., "Bound Populations around cD Galaxies", *The Astrophysical Journal*, vol. 335, 1988, p. 617. doi:10.1086/166953.

Bothun, G. D. and Schombert, J. M., "More Bound Populations around cD Galaxies", *The Astrophysical Journal*, vol. 360, 1990, p. 436. doi:10.1086/169134.

Conselice, C. J., "The Evolution of Galaxy Structure Over Cosmic Time", *Annual Review of Astronomy and Astrophysics*, vol. 52, 2014, pp. 291–337. doi:10.1146/annurev-astro-081913-040037.

Graham, A. W. and Driver, S. P., "A Concise Reference to (Projected) Sérsic $R^{1/n}$ Quantities, Including Concentration, Profile Slopes, Petrosian Indices, and Kron Magnitudes", *Publications of the Astronomical Society of Australia*, vol. 22, no. 2, 2005, pp. 118–127. doi:10.1071/AS05001.

Graham, A. W. and Guzman, R., "On the Unification of Dwarf and Giant Elliptical Galaxies", in *Penetrating Bars Through Masks of Cosmic Dust*, vol. 319, 2004, p. 723. doi:10.1007/978-1-4020-2862-5_62.

Moore, B., Lake, G., and Katz, N., "Morphological Transformation from Galaxy Harassment", *The Astrophysical Journal*, vol. 495, no. 1, 1998, pp. 139–151. doi:10.1086/305264.

Naab, T., Jesseit, R., and Burkert, A., "The Influence of Gas on the Structure of Merger Remnants", *Monthly Notices of the Royal Astronomical Society*, vol. 372, no. 2, 2006, pp. 839–852. doi:10.1111/j.1365-2966.2006.10902.x.

Postman, M., "The Cluster Lensing and Supernova Survey with Hubble: An Overview", *The Astrophysical Journal Supplement Series*, vol. 199, no. 2, 2012. doi:10.1088/0067-0049/199/2/25.

Schombert, J., "Network Tools for Astronomical Data Retrieval", *arXiv e-prints*, 2009. doi:10.48550/arXiv.0910.0896.

Schombert, J. M., "The Structure of Galaxies: II. Fitting Functions and Scaling Relations for Ellipticals", *Publications of the Astronomical Society of Australia*, vol. 30, 2013. doi:10.1017/pas.2013.010.

Schombert, J. M., "The Structure of Galaxies. III. Two Structural Families of Ellipticals", *The Astronomical Journal*, vol. 150, no. 5, 2015. doi:10.1088/0004-6256/150/5/162.